



HAL
open science

Half-Sandwich Nickel(II) NHC-Picolyl Complexes as Catalysts for the Hydrosilylation of Carbonyl Compounds: Evidence for NHC-Nickel Nanoparticles under Harsh Reaction Conditions

Franck Ulm, Saurabh Shahane, Lai Truong-Phuoc, Thierry Romero, Vasiliki Papaefthimiou, Matthieu Chessé, Michael J Chetcuti, Cuong Pham-huu, Christophe Michon, Vincent Ritleng

► To cite this version:

Franck Ulm, Saurabh Shahane, Lai Truong-Phuoc, Thierry Romero, Vasiliki Papaefthimiou, et al.. Half-Sandwich Nickel(II) NHC-Picolyl Complexes as Catalysts for the Hydrosilylation of Carbonyl Compounds: Evidence for NHC-Nickel Nanoparticles under Harsh Reaction Conditions. *European Journal of Inorganic Chemistry*, In press, 2021 (30), pp.3074-3082. 10.1002/ejic.202100371 . hal-03308504

HAL Id: hal-03308504

<https://hal.science/hal-03308504>

Submitted on 29 Jul 2021

HAL is a multi-disciplinary open access archive for the deposit and dissemination of scientific research documents, whether they are published or not. The documents may come from teaching and research institutions in France or abroad, or from public or private research centers.

L'archive ouverte pluridisciplinaire **HAL**, est destinée au dépôt et à la diffusion de documents scientifiques de niveau recherche, publiés ou non, émanant des établissements d'enseignement et de recherche français ou étrangers, des laboratoires publics ou privés.

Half-sandwich nickel(II) NHC-picoyl complexes as catalysts for the hydrosilylation of carbonyl compounds: evidence for NHC-nickel nanoparticles under harsh reaction conditions

Franck Ulm,^[a] Saurabh Shahane,^[a] Lai Truong-Phuoc,^[b] Thierry Romero,^[b]
Vasiliki Papaefthimiou,^[b] Matthieu Chessé,^[a] Michael J. Chetcuti,^{*[a]} Cuong Pham-Huu,^[b]
Christophe Michon^{*[a]} and Vincent Ritleng^{*[a]}

[a] Dr. F. Ulm, Dr. S. Shahane, Mr. M. Chessé, Pr. M. J. Chetcuti, Dr. C. Michon, Pr. V. Ritleng
Université de Strasbourg, Ecole Européenne de Chimie, Polymères et Matériaux, CNRS, LIMA, UMR 7042
25 rue Becquerel, 67087 Strasbourg, France.

E-mail: michael.chetcuti@unistra.fr, cmichon@unistra.fr, vritleng@unistra.fr

[b] Dr. L. Truong-Phuoc, Mr. T. Romero, Dr. V. Papaefthimiou, Dr. C. Pham-Huu
Université de Strasbourg, Institute of Chemistry and Processes for Energy, Environment and Health (ICPEES), UMR 7515 CNRS
25 rue Becquerel, 67087 Strasbourg, France

[c] Dr. C. Pham-Huu, Dr. C. Michon
University of Strasbourg Institute for Advanced Study (USIAS)
5 allée du Général Rouvillois, 67083 Strasbourg, France

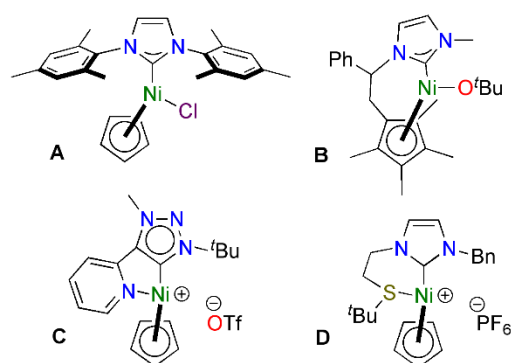
Supporting information for this article is available free of charge on the web.

Abstract: The cationic $[\text{NiCp}(\text{Mes-NHC-CH}_2\text{py})\text{Br}]$ complex **2a** was prepared directly by the reaction of nickelocene with 1-(2-picoyl)-3-mesityl-imidazolium bromide (**1**), and its PF_6^- derivative **2b**, by subsequent salt metathesis. X-Ray diffraction studies and Variable Temperature ^1H NMR experiments run with **2a** and **2b** strongly suggest the bidentate coordination of the picoyl-functionalized carbene to the nickel both in the solid state and in solution in both cases. These data suggest the absence of hemilabile behaviour of the latter, even in the presence of a coordinating anion. Both complexes show similar activity in aldehyde hydrosilylation, further implying the absence of hemilability of the picoyl-functionalized carbene, and effectively reduce a broad scope of aldehydes in the absence of additive under mild conditions. In the case of ketones, effective hydrosilylation is only observed in the presence of a catalytic amount of potassium *t*-butoxide at 100 °C. Dynamic light scattering, scanning transmission electron microscopy and X-ray photoelectron spectroscopy show evidence for the involvement of NHC-picoyl-Ni nanoparticles under these conditions.

Introduction

Hydrosilylation is a reaction of interest for the selective reduction of carbonyl compounds under mild conditions using transition-metal-based catalysts.^[1,2] Indeed, the use of hydrosilanes as reductants, which proceeds without the need of high-pressures or elevated temperatures, is an advantageous surrogate to hydrogenation procedures. As the reactivity of hydrosilanes is modular and depends on their substitution patterns, the hydrosilylation may behave as a highly chemo- and regioselective reduction process that tolerates other reducible functionalities.^[2] Beside catalysts based on noble metals, attention has recently turned to catalysts based on earth-abundant 3d metals, due to sustainability concerns.^[3] Among these developed catalysts,^[4] half-sandwich $[\text{Ni}(\eta^5\text{-C}_5\text{R}_5)\text{L}(\text{NHC})]^{(+)}$ complexes have shown interesting activities for the hydrosilylation of carbonyl derivatives. In 2012, some of us reported that $[\text{NiCpCl}(\text{IMes})]$ **A** ($\text{Cp} = \eta^5\text{-C}_5\text{H}_5$,

$\text{IMes} = 1,3\text{-dimesitylimidazol-2-ylidene}$) effectively catalysed the hydrosilylation of a broad range of aldehydes and ketones at 25 °C in the presence of NaHBEt_3 as a co-catalyst with a turnover frequency (TOF) that reached values up to 390 h^{-1} for the hydrosilylation of benzaldehyde (Scheme 1).^[4e] At the same time, Royo *et al.* described the synthesis of a related half-sandwich nickel(II) complex **B** bearing a bidentate tetramethylcyclopentadienyl-functionalised carbene ligand, $[\text{Ni}(\text{Cp}^*\text{-NHC-Me})(\text{O}^t\text{Bu})]$, that catalysed the reduction of carbonyl derivatives at temperatures ranging from 25 °C (aldehydes) to 100 °C (ketones) with a TOF up to 2 300 h^{-1} for the hydrosilylation of 4-trifluoromethylbenzaldehyde (Scheme 1).^[4f] In 2016, Albrecht *et al.* reported a potentially hemilabile pyridyl-triazolylidene NiCp precatalyst **C** for the hydrosilylation of aldehydes with a TOF as high as 13 350 h^{-1} observed with 4-methoxybenzaldehyde at 60 °C (Scheme 1).^[4w]



Scheme 1. Previously reported $[\text{Ni}(\eta^5\text{-C}_5\text{R}_5)\text{L}(\text{NHC})]^{(+)}$ precatalysts for the hydrosilylation of carbonyl compounds.

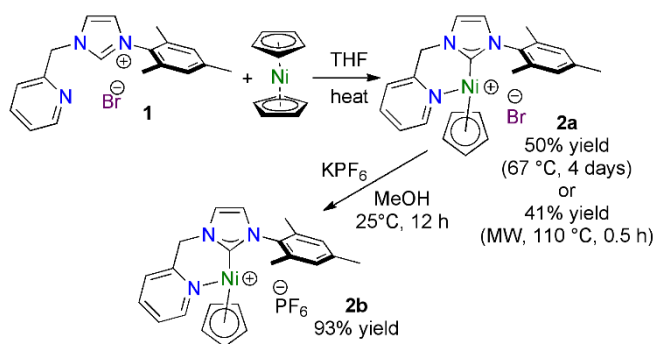
The high TOF observed with the latter complex was tentatively rationalized as the result a well-balanced hemilabile ligand, with a C,N-chelate that can both stabilize the catalyst by a strong

bidentate chelation in the resting state and enable an effective reactivity at the nickel centre by ring opening on the substrate's approach.^[4w] The hemilabile balance of chelates may indeed be of utmost importance to develop efficient catalysts. This is especially true for $[\text{Ni}(\eta^5\text{-C}_5\text{R}_5)(\text{NHC-Y})]^{(+)}$ complexes, which do not have potentially available coordination site aside from those resulting from decoordination of the Lewis basic Y atom and/or Cp ring slippage from η^5 - to η^3 - or even η^1 - or decoordination.^[5,6] Following a recent work in our group on nickel complexes such as **D** (Scheme 1) bearing hemilabile $\kappa^2\text{-C,S}$ -thioether-functionalised NHCs,^[7] we wondered whether a NHC-picoyl ligand could afford a suitable balance in such type of complexes for nickel-catalysed hydrosilylation reactions.

Herein we describe the synthesis of the cationic $[\text{NiCp}(\text{Mes-NHC-CH}_2\text{py})\text{Br}]$ complex bearing a $\kappa^2\text{-C,N}$ -1-(2-picoyl)-3-mesityl-imidazol-2-ylidene ligand directly from nickelocene and the corresponding imidazolium bromide. X-Ray diffraction and Variable Temperature (VT) ^1H NMR studies strongly suggest the preferential coordination of the pyridine side arm over the bromide anion, both in solution and in the solid state, therefore suggesting no hemilabile behaviour of the picoyl-functionalized carbene ligand. The latter complex and its PF_6^- derivative obtained by salt metathesis show similar activity in aldehyde hydrosilylation under mild conditions, which further suggests the absence of hemilabile behaviour. In the case of ketones, the addition $\text{KO}t\text{Bu}$ to the catalytic medium and a temperature of 100 °C are requested to observe effective reductions. Diffusion Light Scattering (DLS), Scanning Electron Microscopy in the Transmission mode (SEM-T) and X-ray Photoelectron Spectroscopy (XPS) show evidence for the involvement of NHC-Ni nanoparticles under these conditions.

Results and Discussion

Our investigations started with the synthesis of complex **2a** by the reaction of the imidazolium bromide **1**^[8] with nickelocene in THF under reflux (Scheme 2). The use of a conventional oil bath heater resulted in the obtention of **2a** with a 50% yield after 4 days. Heating through microwave (2.45 GHz) at 110 °C allowed a substantial reduction in the reaction time, affording **2a** in 41% yield after just 0.5 h. In contrast to what was observed for the reactions of nickelocene with thioether-functionalized imidazo-



Scheme 2. Synthesis of the cationic NHC-picoyl-Ni(II) complexes **2a** and **2b**.

lium bromides that yielded neutral complexes bearing monodentate carbenes,^[7] the bromide anion was found uncoordinated, and a cationic species bearing a $\kappa^2\text{-C,N}$ -picoyl-NHC ligand was obtained. The subsequent metathesis of Br to PF_6^- anion led to complex **2b** with a 93% yield. It is noteworthy that the synthesis of the BF_4^- analogue of **2a** and **2b** was recently reported by Valerga *et al.* through a two-step procedure involving reaction of **1** with Ag_2O and subsequent transmetalation to nickel by reaction with the air-sensitive $[\text{NiCp}(\text{COD})](\text{BF}_4)$.^[5b]

Single crystals of **2a** and **2b** were obtained at -28 °C by diffusion of *n*-pentane in a THF solution of **2a** and by slow solvent evaporation from a solution of **2b** in chloroform. X-ray diffraction studies of **2a** and **2b** established the molecular structures and $\kappa^2\text{-C,N}$ -coordination pattern of the 1-(2-picoyl)-3-mesityl-imidazol-2-ylidene ligand for both complexes in the solid state (Figures 1, S1-S4). Key bond distances and angles are listed in Table 1 and selected crystallographic data and data collection parameters can be found in Table S1.

Complex **2a** crystallizes in the orthorhombic space group $\text{P}2_12_12_1$. The coordination of the Ni atom is characterized by a Ni–C(1) bond distance of 1.864 Å, a Ni–N(3) distance of 1.922 Å and a Ni–Cp_{cent} distance of 1.751 Å (Table 1) [C(1) = the carbene carbon atom]. The corresponding Ni···Br anion distance is 7.528 Å. Whereas C(1)–Ni–N(3) bite angle is orthogonal with a value of 91.5°, C(1)–Ni–Cp_{cent} and N(3)–Ni–Cp_{cent} angles are larger at 134.6° and 133.9°, respectively. This is characteristic of $[\text{Ni}(\eta^5\text{-C}_5\text{R}_5)(\text{NHC})\text{L}]^{(+)}$ type complexes.^[5b,7,9] One can note however the

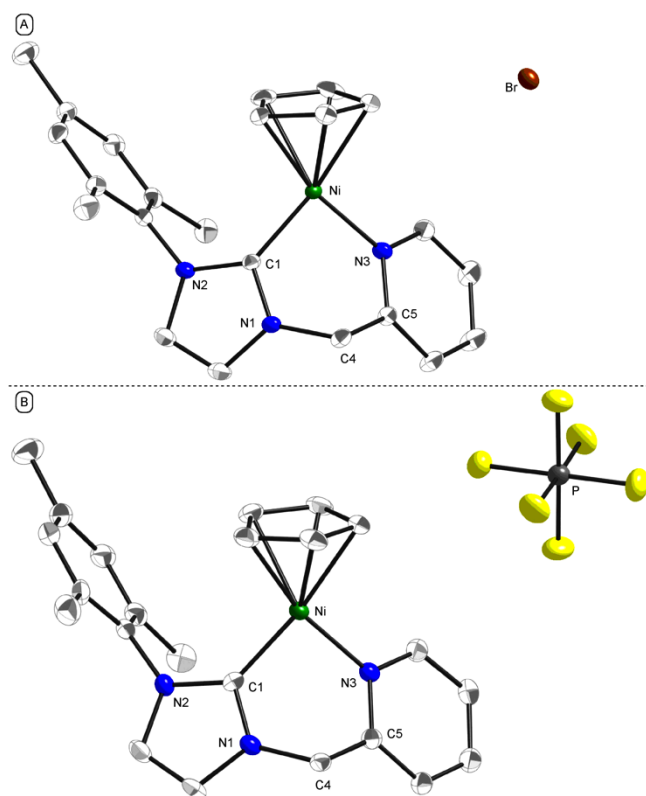


Figure 1. (A) Molecular structure of complex **2a** showing all non-H atoms of the cation and one Br⁻ anion. (B) Molecular structure of complex **2b** showing all non-H atoms of cation **2b**¹⁺ and one PF_6^- anion. Disorder on the latter, one molecule of CHCl_3 and another complex were deleted for clarity. Ellipsoids are shown at the 50% probability level, and key atoms are labelled.^[10]

Table 1. Selected distances (Å) and angles (°) in **2a**, **2b₁** and **2b₂** with esd's in parentheses

	2a	2b₁	2b₂
Ni–C(1)	1.864(3)	1.875(5)	1.875(5)
Ni–N(3)	1.922(3)	1.930(4)	1.916(4)
Ni–C _{pcent} [a]	1.751	1.747	1.745
Ni–C _{cp} av [b]	2.124	2.119	2.121
C(1)–Ni–N(3)	91.5(1)	92.9(2)	92.2(2)
C(1)–Ni–C _{pcent}	134.6	133.9	133.8
N(3)–Ni–C _{pcent}	133.9	133.2	133.8

[a] C_{pcent} = centroid of the Cp group. [b] Average Ni–C distance to the Cp ring.

relatively smaller C(1)–Ni–N(3) bite angle of **2a** compared to the corresponding C(1)–Ni–S and C(1)–Ni–C angles of the κ^2 -C,S-NHC-thioether complex **D** (95.94°)^[7] and of a related κ^2 -C,C-6-membered half-sandwich nickelacycle (94.0°).^[9d] Similar values (89.5–91.7°) were observed in the NiCp and NiCp* (Cp* = η^5 -C₅Me₅) complexes described by Valerga *et al.*, bearing closely related κ^2 -C,N-picolylimidazol-2-ylidene ligands.^[5b]

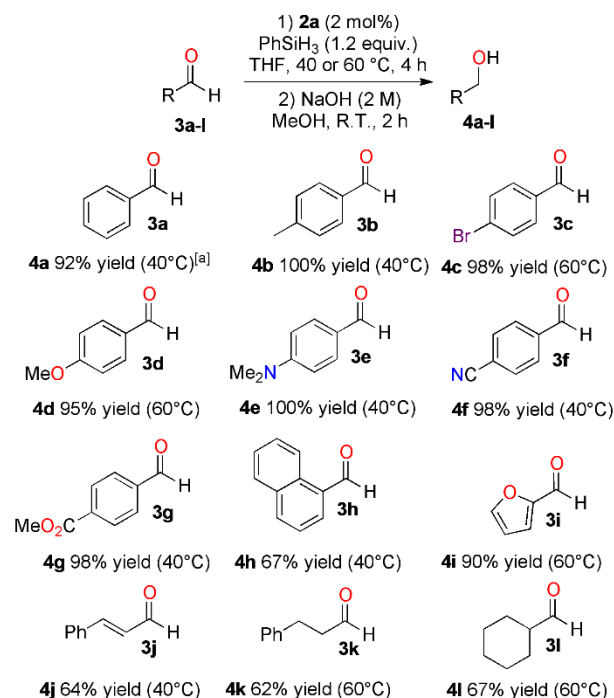
By comparison, complex **2b** crystallizes in the triclinic space group *P*1, with two independent cations, **2b₁**⁺ and **2b₂**⁺, two PF₆[−] anions and one molecule of chloroform in the crystal unit cell (Figures 1B, S3–S4). The cations **2b₁**⁺ and **2b₂**⁺ are not identical having slightly different structural parameters (Table 1) and the fluorine atoms of one PF₆[−] anion exhibit some disorder over two positions. Thus, the coordination of the Ni atoms in **2b₁**⁺ and **2b₂**⁺ is characterized by the following distances: Ni–C(1) = 1.875/1.875 Å, Ni–N(3) = 1.930/1.916 Å and Ni–C_{pcent} = 1.747/1.745 Å (Table 1). Stronger similarities are noteworthy for the C(1)–Ni–N(3) bite angles with 92.9 and 92.2°, the C(1)–Ni–C_{pcent} angles with 133.9 and 133.8° and the N(3)–Ni–C_{pcent} angles with 133.2 and 133.8°, respectively.

The main spectroscopic features of **2a,b** are in agreement with their X-ray structures. The carbene carbon is observed at ca. 162 ppm in the ¹³C NMR (CDCl₃) spectra while the Cp carbons appear at ca. 92.5 ppm. In the ¹H NMR spectra, the Cp protons of **2a** and **2b** resonate as a singlet at 4.99 ppm in both cases. However, in contrast to what is expected in the case of a chelate, the ¹H NMR spectrum of **2a** at room temperature (RT) exhibits a broad singlet at 6.32 ppm that integrates for two protons for the methylene protons. Similarly, the ¹H NMR spectrum of **2b** at RT shows these protons as a singlet integrating for two protons, however as a sharper and slightly more shielded (5.68 ppm) peak in this case. These surprising observations suggested the existence of a dynamic process in solution at RT in both complexes. VT ¹H NMR experiments were then performed on CD₂Cl₂ solutions of **2a** and **2b** between 298 and 203 K to check if these dynamic processes could be frozen on the NMR time scale at low temperature. In the case of **2a**, the singlet of the NCH₂py methylene group that is observed at 5.56 ppm at 298 K in CD₂Cl₂ broadens as the temperature decreases and decoalesces between 213 and 208 K to give two very broad signals integrating for one proton each at 5.47 and 5.43 ppm at 203 K. The free energy of activation (ΔG^\ddagger) for this process, based on this (de)coalescence temperature of the NCH₂py group (ca. 210 K) is of ca. 16 kcal mol^{−1}.^[11] In contrast, no decoalescence could be

observed for **2b**, indicating a fast dynamic process involving the NCH₂py arm on the NMR time scale. Considering the weak coordinating ability of the PF₆[−] anion, it is unlikely that the latter can displace the pyridine group from the nickel centre. Thus, it is reasonable to postulate that the absence of diastereotopy observed for **2b**, even at low temperature, is likely due to small angle oscillations about the N3–Ni and N1–C1 bonds, and/or to conformational isomerization of the “chair–boat” type as proposed by Valerga *et al.* for closely related κ^2 -C,N-[Ni(η^5 -C₅R₅)(Ar-NHC-CH₂-Py)](BF₄) complexes. In the case of **2a**, a similar process most probably occurs as the decoalescence of the methylene signal observed at low temperature strongly suggest the coordination of the pyridyl group to the nickel centre in solution as well.^[12] This assumption is further corroborated by the green colour of the solution, characteristic of cationic [Ni(η^5 -C₅R₅)L(NHC)]⁺X[−] complexes,^[7,12] as well as by the chemical shift of the pyridine nitrogen atom at 217 ppm in the ¹⁵N NMR spectrum of **2a** at 298 K (Figure S5), characteristic of pyridine nitrogen atom coordination to a metal centre.^[13]

Complexes **2a,b** were subsequently applied as catalysts for the reduction of benzaldehyde **3a** to benzylic alcohol **4a** through hydrosilylation using solely phenyl silane, and subsequent basic hydrolysis (Scheme 3). At a loading of 2 mol% under mild reaction conditions (e.g. 4 h at 40 °C), complexes **2a** and **2b** both allowed the effective reduction of **3a** into **4a** with a similar yield of 92%, thus showing no difference of reactivity despite the different coordinating ability of their respective counter-ions.

The substrate scope of the reaction was then explored investigating the hydrosilylation of substituted benzaldehydes **3b–g** to the corresponding alcohols **4b–g** (Scheme 3). By using **2a** as catalyst and similar conditions, these reactions also proceeded in high yields independently of the electron-donor or



Scheme 3. Hydrosilylation of aldehydes **3a–l** to alcohols **4a–l** using catalyst **2a**. NMR yields (%). [a] Same result using catalyst **2b**.

-acceptor character of the substituents. It is worth noting that substrates **3c** and **3d** bearing bromo or methoxy groups required heating to 60 °C in order to proceed smoothly. Interestingly, the hydrosilylation of aldehydes **3f** and **3g** proceeded chemoselectively, the nitrile and ester functions being not reduced. In addition, 1-napthaldehyde **3h** and furan-2-carbaldehyde **3i** were effectively converted to the corresponding alcohols in 67% and 90% yields, respectively (Scheme 3). Finally, the hydrosilylation of **3l** proceeded at 40 °C with a 64% yield and without any reduction of the conjugated C=C double bond. By comparison, the reaction of alkyl aldehydes **3k** and **3l** required a 60 °C heating in order to afford similar yields.

We next focused our attention on the catalytic activity of complexes **2a,b** for the hydrosilylation of acetophenone **5a** (Table 2). By using similar reaction conditions as for the reduction of aldehydes (e.g. 40 °C, 4 h), the catalysts **2a,b** again showed a similar activity, leading to the corresponding alcohol **6a** in a similar 16% yield (entries 1-2). The latter was slightly increased to 25% by heating at 60 °C for 19 h (entry 3). In order to check the effect of the counter-anion and various additives on the catalysis,^[14] an anion screening was carried out (entries 4-10). Apart from acetate that led to a 21% yield for **6a** after 4 h reaction at 40 °C (entry 10), none of the BArF₂₄⁻ (tetrakis[3,5-

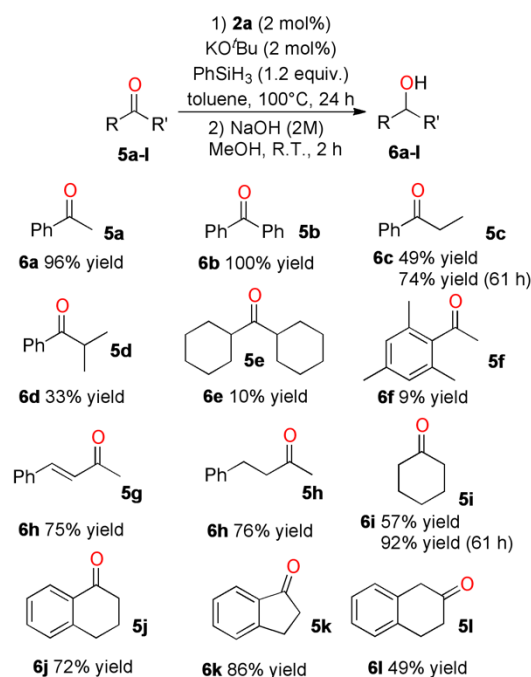
trifluoromethyl)phenyl]borate), SbF₆⁻, OTf⁻, NTf₂⁻ or acac⁻ anions afforded a better yield than **2a,b** without additives (entries 4-9). An increase of the reaction temperature to 60 °C and time to 19 h resulted in a 38% yield of **6a** with KOAc (entry 11). A similar trend was observed with KO^tBu as additive (entries 12 and 13),^[4f,15,16] but a higher yield of 47% yield was obtained (entry 13), though this additive effect was not significant at 40 °C (entry 12). A change of solvent to toluene allowed a further increase of the reaction temperature to 100 °C and afforded benzyl alcohol **6a** with a 74% yield in 19 h and an almost quantitative 96 % yield in 24 h (entries 14-16).

With these conditions in hand, the substrate scope of the reaction was then explored by investigating the hydrosilylation of various aryl and alkyl ketones **5a-l** into the corresponding alcohols **6a-l** (Scheme 4). Though the hydrosilylation of acetophenone **5a** and benzophenone **5b** proceeded in high yields, the reduction of propiophenone **5c** proved to be harder, a reaction time of 61 h being required in order to reach 74% yield. Moreover, the hydrosilylation of more sterically hindered ketones was limited.^[17] Indeed, the reductions of 2-methyl-1-phenylpropan-1-one **5d**, dicyclohexylmethanone **5e** and 2-acetylmethylstyrene **5f** led to much lower yields. Furthermore, it is worth noting that the hydrosilylation of the conjugated ketone, 4-phenylbut-3-en-2-one **5g**, proceeded with 75% yield in 24 h and implied the reduction of both the carbonyl and the conjugated C=C double bond, thus leading to the saturated alcohol **6h**. By comparison, the reduction of 4-phenylbutan-2-one **5h** led to **6h** in a similar yield. The hydrosilylation of cyclohexanone **5i** afforded the corresponding cyclohexanol **6i** in 57% yield after 24 h reaction, but an extended reaction time to 61 h resulted in 92% yield. The reduction of other cyclic ketones **5j-l** comprising an additional aromatic proceeded in moderate to good yields.

Table 2. Reaction conditions optimization for the hydrosilylation of acetophenone **5a**^[a]

Ent.	Cat.	Solvent	Additive (mol%)	T (°C)	Time (h)	Yield (%) ^[b]
1	2a	THF	-	40	4	16
2	2b	THF	-	40	4	16
3	2a	THF	-	60	19	25
4	2a	THF	NaSbF ₆ (2)	40	4	6
5	2a	THF	NaBArF ₂₄ (2)	40	4	6
6	2a	THF	KBArF ₂₄ (2)	40	4	1
7	2a	THF	NBu ₄ OTf (2)	40	4	1
8	2a	THF	KNTf ₂ (2)	40	4	7
9	2a	THF	Kacac (4)	40	4	10
10	2a	THF	KOAc (4)	40	4	21
11	2a	THF	KOAc (4)	60	19	38
12	2a	THF	KO ^t Bu (2)	40	4	15
13	2a	THF	KO ^t Bu (2)	60	19	47
14	2a	Toluene	KO ^t Bu (2)	60	19	49
15	2a	Toluene	KO ^t Bu (2)	100	19	74 ^[c]
16	2a	Toluene	KO ^t Bu (2)	100	24	96

[a] Experiments run on a 0.25 mmol acetophenone scale. [b] Isolated yields after hydrolysis. [c] 22% yield without KO^tBu additive.



Scheme 4. Hydrosilylation of ketones **5a-l** into alcohols **6a-l** using catalyst **2a**. GC yields (%).

Regarding the activation effect of KO t Bu^[15,16,18] and the reaction mechanism at play in these ketones' hydrosilylations, it is of interest that the reductions of **5a-I** were characterized by a striking colour change from clear brown to deep black within a few minutes (Figures S6 and S7). To gain some insight into the nature of the active species, we prepared a toluene- d_8 solution comprising complex **2a** (2 mol%), KO t Bu (2 mol%) and phenylsilane, but without the ketone reagent, and heated up to 100 °C for 1 h. The same colour change was observed. After cooling the reaction medium to room temperature, a sample was placed in a sealed tube and analysed by ¹H and ²⁹Si NMR spectroscopy. The resulting ¹H NMR spectrum did not show any hydride intermediate^[4e,18,19] nor any [Ni(I)Cp(NHC)]^[18,20] or other well-defined Ni species, and further interpretations proved to be difficult. The ²⁹Si NMR spectrum did not allow us to observe the pentacoordinate siliconate species, [PhSiH₃(O t Bu)]⁻ (at $\delta^{29}\text{Si} = -96.2$ ppm), that was reported by Thomas *et al.* to act as an *in situ* generated universal reducing species of a relatively wide range of pre-catalysts of Fe(II), Co(II) and Mn(II) for hydrosilylation reactions when NaO t Bu was used as an activator in conjunction with PhSiH₃.^[15]

Despite the change of colour to deep black, the course of the catalytic reduction of acetophenone under the conditions of Scheme 4 remained unchanged when performing a hot filtration test after 19 h reaction, and similarly afforded **6a** in 96% yield after 24 h reaction. Furthermore analyses of both a sample of **2a** (2 mol%), KO t Bu (2 mol%) and PhSiH₃ and a sample of **2a** (2 mol%) and PhSiH₃, prepared in toluene at 100 °C, by GC-MS and IR spectroscopy showed no evidence of NHC ligand degradation to the corresponding azolone (Figures S8-S14), therefore allowing us to rule out an Ananikov type activation/deactivation mechanism.^[16] Nevertheless, when we performed a measurement by DLS^[21] on a similar sample of **2a** (2 mol%), KO t Bu (2 mol%) and PhSiH₃ prepared in toluene at 100 °C, we observed a fine distribution of particles of ca. 310 nm wide (Figure S15). To establish whether these particles were generated by the combined action of PhSiH₃ and KO t Bu at 100 °C or the sole action of PhSiH₃ at this temperature, we next prepared a sample from complex **2a** and PhSiH₃ in toluene under similar conditions, but without addition of KO t Bu. DLS indicated the presence of nanoparticles of average 90 nm sizes in this case (Figures S16). However, these nanoparticles proved to be relatively ineffective for the hydrosilylation of acetophenone **5a** compared to the particles generated in the presence of KO t Bu (22% yield after 19 h at 100 °C vs. 74% yield in the presence of KO t Bu, see Table 2, entry 15).

Afterwards, we evaporated a DLS sample of **2a** (2 mol%), KO t Bu (2 mol%) and PhSiH₃ prepared in toluene at 100 °C on a glass support in an argon filled glovebox; the remaining oily solid residue was subsequently analysed by X-ray diffraction (XRD) in the reflexion mode (Figures S17 and S18). Most of the observed diffractions were fitted with the diffraction patterns of KBr. Such a result can be attributed to the poor crystallinity of the sample. This rendered the observation of NiO (most probably formed after air exposure) difficult, and there was no evidence for the presence of Ni(111), e.g. Ni(0) species. However, XRD is mainly a bulk technique, which is hardly accurate for the analysis of such small and dispersed samples.

Two similar samples, one fresh and one aged, were then analysed by XPS in order to determine the chemical composition at the topmost surface (*i.e.*: 9 ± 2 nm) of the catalysts. The survey

scan and high-resolution spectra of the freshly prepared sample revealed the core levels of C1s, O1s, N1s, Ni2p, Br3d and Si2p elements (Figures S19 and S20). More specifically, the peaks values for Ni2p_{3/2} and 2p_{3/2} satellite of the Ni2p region are found at 853.6 and ca. 861.7 eV, respectively (Figure 2, red). These values are consistent with the presence of NiO, which could result from the oxidation of the Ni(0) species during the transport of the sample in air, as observed by XRD. However, it is worthy to note that, due to the weak signal-to-noise ratio, the assignment of the Ni(0) vs. Ni(2+) is not straightforward, and the presence of some residual Ni(0) cannot be completely ruled out in this sample (Figures S20 and S21).^[22] Raman spectroscopy, carried out on a sample whose exposure to air was avoided, indeed showed no evidence of Ni oxides (150-430 cm⁻¹) and Ni hydroxides (3100-3650 cm⁻¹) (Figure S22).

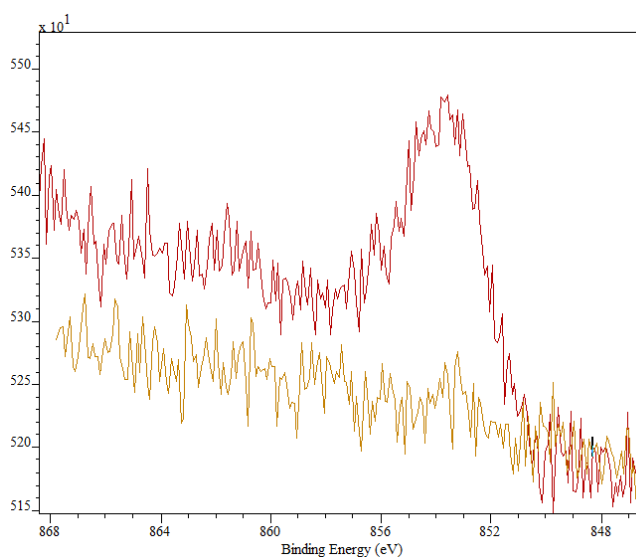


Figure 2. XPS spectra of Ni 2p_{3/2}. Red: fresh sample; orange: aged sample.

Interestingly, no Ni was detected by XPS in the aged sample (Figure 2, orange), suggesting the progressive agglomeration of the nanoparticles (filtration onto 200 nm PTFE filters was carried out before analysis), and thus their instability. Furthermore, the % surface ratio of all the elements confirmed the presence of C, O, N, Si, Br and Ni elements in the fresh sample and the Ni/N ratio of 1:4 suggested the presence of NHC-picolyl-coordinated Ni particles. As expected, the old sample contained only C, O, N and Si elements (Table S3).

Evaporation in an argon filled glovebox of a similar sample of **2a** (2 mol%), KO t Bu (2 mol%) and PhSiH₃ on a membrane support allowed analyses by SEM and SEM-T microscopies. Some faceted particles with a dimension of ca. 200 to 600 nm were observed which could be attributed to the Ni-based material (Figures 3 and S22). SEM-EDX chemical analysis confirmed that the observed particles were comprised of C, N, O, Ni, Br and Si elements, at least on their surface (Figure S23, Table S3). To get further insight into the bulk composition of these 310 nm particles and get a reliable estimation of the number of NHC-picolyl ligands that remain bound to the nickel, two samples were then analysed by ICP-AES and CHN elemental analyses. Mass percentages of 6.3 ± 0.2 (Ni) and 3.16 ± 0.4 (N) were measured, which corresponds to a Ni:N molar ratio of 1:2, thus to a Ni:NHC ratio of 1.5:1. These results confirm the coordination of NHC-picolyl

ligands to the Ni nanoparticles and highlight, to the best of our knowledge, only the third example of NHC stabilized nanoparticles.^[23,24]

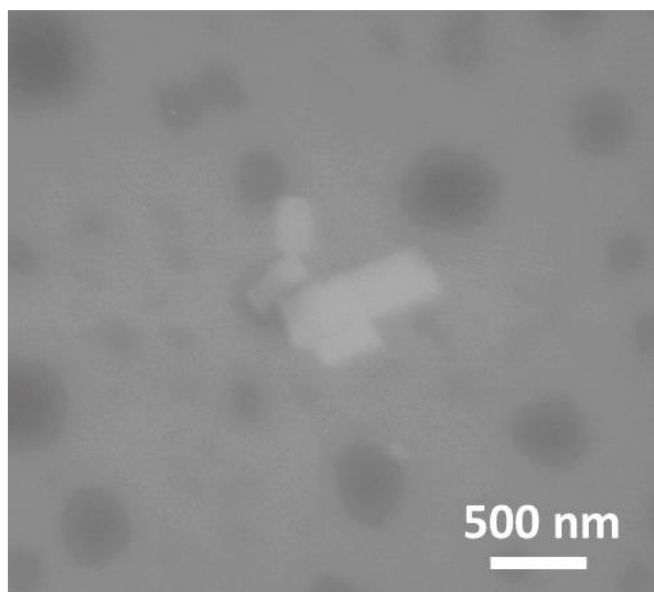


Figure 3. MEB-STEM image of Ni NHC-picolyli nanoparticles.

Conclusion

In this work, we have shown that an accessible cationic half-sandwich Ni(II)-NHC-picolyli complex **2a** bearing a bromide counter-ion effectively catalyzes the hydrosilylation of a broad range of aldehydes without additive and of ketones in the presence of KO^tBu at 100 °C. Single-crystal and VT ¹H NMR studies tend to show the absence of a hemilability of the picolyli-functionalized carbene ligand. Studies by DLS, transmission mode SEM, XPS, ICP-AES and CHN elemental analyses showed evidence for the involvement of NHC-picolyli Ni particles in the catalytic reactions when KO^tBu is used as an additive. Though KO^tBu clearly acts as an activator leading to the formation of catalytically active particles, together with PhSiH₃, their detailed implication in this process remains unclear. Further studies on such NHC-stabilized-Ni nanocatalysts are currently in progress in our laboratories and will be reported in the future.

Experimental Section

Synthesis of [NiCp{Bn-NHC-(CH₂)-Py}](Br) (**2a**)

A 10 mL vial containing a stirring bar was charged with nickelocene (106 mg, 0.561 mmol), 1-mesityl-3-(2-picolyli)imidazolium bromide **1** (200 mg, 0.558 mmol), and THF (5 mL). After sealing the vial, the green suspension was heated at 110 °C for 0.5 h in a Discover CEM S-class microwave operating at 2.45 GHz. The resulting suspension was filtered through a Celite pad that was washed with THF (3 x 10 mL). The solvent was then removed under vacuum, and the resulting residue triturated in pentane (5 mL) to afford **2a** as a green powder after solvent removal with a syringe and vacuum drying (109 mg, 0.223 mmol, 41 % yield). Anal. calcd for C₂₃H₂₄BrN₃Ni: C, 57.43; H, 5.03; N, 8.74; found: C, 57.12; H, 4.96; N, 8.81. ESI-MS (TOF): m/z 400.1318 calcd. for C₂₃H₂₄N₃Ni [M-Br]⁺, 400.1318, found 400.1298. ¹H NMR (CDCl₃, 300 MHz): δ 8.61 (s, 1 H, NCH), 8.51 (br. d, ³J = 7.5, 1H, 3- or 6-H_{Py}), 8.30 (d, ³J = 5.4, 1H, 3- or 6-H_{Py}), 7.84 (t, ³J = 7.5, 1H, 4- or 5-H_{Py}), 7.08 (t, ³J = 5.1, 1H, 4- or 5-H_{Py}), 7.05 (s, 2H, m-H_{Mes}), 6.75 (s, 1H, NCH), 6.32 (s, 2H, CH₂), 4.99 (s, 5H, C₅H₅), 2.39 (s, 3H,

p-CH₃), 2.03 (s, 6H, *o*-CH₃). ¹³C{¹H} NMR (CDCl₃, 75 MHz): δ 161.0 (NCN), 158.3 (3-C_{Py}), 157.1 (1-C_{Py}), 140.1 (*ipso*-C_{Mes}), 139.4 (5-C_{Py}), 135.6 (*p*-C_{Mes}), 135.2 (*o*-C_{Mes}), 129.5 (*m*-C_{Mes}), 128.1 (6-C_{Py}), 126.1 (4-C_{Py}), 124.2 (NCH), 122.9 (NCH), 92.4 (C₅H₅), 53.8 (CH₂), 21.3 (*p*-CH₃), 18.2 (*o*-CH₃).

Synthesis of [NiCp{Bn-NHC-(CH₂)-Py}](PF₆) (**2b**)

An oven dried Schlenk tube containing a stirring bar was loaded with **2a** (300 mg, 0.624 mmol), KPF₆ (0.115 mg, 0.625 mmol) and THF (4 mL). The resulting green suspension was stirred at room temperature overnight and at 40 °C for 40 min. The reaction medium was then cooled to room temperature and its contents filtered over a pad of Celite that was washed with THF until the solvent went colourless. The filtrate was evaporated to dryness to give **2b** as a green powder (338 mg, 0.619 mmol, 93% yield). Anal. calcd for C₂₃H₂₄F₆N₃NiP + ½ C₄H₈O: C, 51.57; H, 4.85; N, 7.22; found: C, 51.48; H, 5.01; N, 6.95. ESI-MS (TOF): m/z 400.1318 calcd. for C₂₃H₂₄N₃Ni [M-PF₆]⁺, found 400.1310. ¹H NMR (CDCl₃, 300 MHz): δ 8.36 (d, ³J = 5.7, 1H, 3-H_{Py}), 7.89 (m, 1H, 4- or 5-H_{Py}), 7.85 (dd, ³J = 7.5, ⁴J = 1.5, 1H, 6-H_{Py}), 7.82 (d, ³J = 1.8, 1H, NCH), 7.12 (ddd, ³J = 7.2, ³J = 5.7, ⁴J = 1.5, 1H, 4- or 5-H_{Py}), 7.06 (s, 2H, *m*-H_{Mes}), 6.80 (d, ³J = 1.8, 1H, NCH), 5.68 (s, 2H, CH₂), 4.99 (s, 5H, C₅H₅), 2.39 (s, 3H, *p*-CH₃), 2.05 (s, 6H, *o*-CH₃). ¹³C{¹H} NMR (CDCl₃, 75 MHz): δ 162.5 (NCN), 158.8 (3-C_{Py}), 156.2 (1-C_{Py}), 140.2 (*ipso*-C_{Mes}), 139.5 (5-C_{Py}), 135.4 (*p*-C_{Mes}), 135.2 (*o*-C_{Mes}), 129.6 (*m*-C_{Mes}), 126.9 (6-C_{Py}), 125.0 (4-C_{Py}), 124.6 (NCH), 123.4 (NCH), 92.6 (C₅H₅), 54.4 (CH₂), 21.3 (*p*-CH₃), 18.1 (*o*-CH₃).

General procedure for the hydrosilylation of aldehydes **3** into alcohols **4**

An oven dried Schlenk tube containing a stirring bar was loaded with the nickel pre-catalyst **2a** (9.6 mg, 0.02 mmol) and dry THF (4 mL). To the resulting green solution was added the aldehyde (1.00 mmol) and PhSiH₃ (148 μL, 1.20 mmol), in this order, and the reaction mixture was stirred in a preheated oil bath at 40 °C for 4 h. The reaction mixture was then quenched by the addition of methanol (2 mL) and 2 M NaOH (2 mL) and stirred for 2 h. After the addition of water (5 mL), the product was extracted with diethylether (3 x 10 mL). The combined organic layers were dried over anhydrous MgSO₄, filtered and concentrated under vacuum. The conversion was determined by ¹H NMR spectroscopy, and the product purified by flash chromatography on silica gel using petroleum ether/diethyl ether (80:20 and 50:50) mixtures. All conversions and yields are the average value of at least two runs.

General procedure for the hydrosilylation of ketones **5** into alcohols **6**.

An oven dried Schlenk tube containing a stirring bar was loaded with the nickel pre-catalyst **2a** (4.8 mg, 0.01 mmol), KO^tBu (1.1 mg, 0.01 mmol) and dry toluene (2 mL). To the resulting deep orange solution was added the ketone (0.5 mmol) and PhSiH₃ (74 μL, 0.6 mmol), in this order, and the reaction mixture was stirred in a preheated oil bath at 100 °C for 24 h. The reaction mixture was then quenched by the addition of methanol (2 mL) and 2 M NaOH (2 mL) and stirred for 2 h. After the addition of water (5 mL), the product was extracted with diethylether (3 x 10 mL). The combined organic layers were dried over anhydrous MgSO₄, filtered and concentrated under vacuum. The conversion was determined by ¹H NMR spectroscopy and GC analysis, and the product purified by flash chromatography on silica gel using petroleum ether / ethyl acetate (80:20 and 50:50) mixtures. All conversions and yields are the average value of at least two runs.

Acknowledgements

The CNRS, the University of Strasbourg, and the Agence Nationale de la Recherche (ANR 2010 JJC 716 1) are acknowledged for supporting and funding partially this work (post-doc of S. Shahane). The Institut Universitaire de France is acknowledged for its support (V.R.), and the Région Grand Est for the doctoral fellowship of F. Ulm. This work has also benefitted from support provided by the University of Strasbourg Institute for Advanced Study (USIAS) for a Fellowship, within the French national program "Investment for the future" (IdEx-Unistra) (C.M. and C.P.-H.). Mrs. Corinne Bailly and Dr. Lydia Karmazin are acknowledged for the X-ray structural determinations. Mrs. Alexandra Sutter (ICPEES) is gratefully thanked for her assistance with DLS measurements and discussion. Dr. Emeric

Wasielowski (LIMA) is thanked for his assistance with NMR experiments.

Keywords: Carbonyls • Hydrosilylation • N-heterocyclic carbenes • Nanoparticles • Nickel

- [1] a) P. G. Andersson, I. J. Munslow (Eds.), *Modern Reduction Methods*, Wiley, New York, **2008**; b) P. A. Dub, T. Ikariya, *ACS Catal.* **2012**, *2*, 1718–1741; c) J. March, *Advanced Organic Chemistry: Reactions, Mechanisms and Structures, Seventh Edition*, Wiley-VCH, New York, **2013**.
- [2] a) B. Marciniak, H. Maciejewski, C. Pietraszuk, P. Pawluć in *Hydrosilylation: A Comprehensive Review on Recent Advances* (Ed. B. Marciniak), Springer, Heidelberg, **2009**; b) D. Addis, S. Das, K. Junge, M. Beller, *Angew. Chem. Int. Ed.* **2011**, *50*, 6004–6011; *Angew. Chem.* **2011**, *123*, 6128–6135; c) S. Werkmeister, K. Junge, M. Beller, *Org. Process Res. Dev.* **2014**, *18*, 289–302; d) K. Revunova, G. I. Nikonov, *Dalton Trans.* **2015**, *44*, 840–866; e) J. Pesti, G. L. Larson, *Org. Process Res. Dev.* **2016**, *20*, 1164–1181; f) M. Oestreich, *Angew. Chem. Int. Ed.* **2016**, *55*, 494–499; *Angew. Chem.* **2016**, *128*, 504; g) M. C. Lipke, A. L. Liberman-Martin, T. D. Tilley, *Angew. Chem. Int. Ed.* **2017**, *56*, 2260–2294; *Angew. Chem.* **2017**, *129*, 2298–2332.
- [3] a) A. Correa, O. G. Mancheno, C. Bolm, *Chem. Soc. Rev.* **2008**, *37*, 1108–1117; b) C. Wang, X. F. Wu, J. L. Xiao, *Chem. Asian J.* **2008**, *3*, 1750–1770; c) P. J. Chirik, in: *Catalysis without Precious Metals*, Wiley-VCH, 2010, pp. 83–110; d) M. S. Holzwarth, B. Plietker, *ChemCatChem* **2013**, *5*, 1650–1679; e) R. M. Bullock, *Science* **2013**, *342*, 1054–1055; f) S. W. M. Crossley, C. Obradors, R. M. Martinez, R. A. Shenvi, *Chem. Rev.* **2016**, *116*, 8912–9000; g) J. R. Ludwig, C. S. Schindler, *Chem* **2017**, *2*, 313–316.
- [4] Hydrosilylation of aldehydes and ketones using first-row transition metals (Mn, Fe, Co, Ni, Cu), see: a) F. Jiang, D. Bezier, J.-B. Sortais, C. Darcel, *Adv. Synth. Catal.* **2011**, *353*, 239–244; b) L. C. Misal Castro, D. Bezier, J.-B. Sortais, C. Darcel, *Adv. Synth. Catal.* **2011**, *353*, 1279–1284; c) E. Buitrago, F. Tinnis, H. Adolfsen, *Adv. Synth. Catal.* **2012**, *354*, 217–222; d) D. Bezier, F. Jiang, T. Roisnel, J.-B. Sortais, C. Darcel, *Eur. J. Inorg. Chem.* **2012**, 1333–1337; e) L. P. Bheeter, M. Henrion, L. Brelot, C. Darcel, M. J. Chetcuti, J.-B. Sortais, V. Ritleng, *Adv. Synth. Catal.* **2012**, *354*, 2619–2624; f) L. Postigo, B. Royo, *Adv. Synth. Catal.* **2012**, *354*, 2613–2618; g) J. Zheng, C. Darcel, J.-B. Sortais, *Catal. Sci. Technol.* **2013**, *3*, 81–84; h) A. J. Ruddy, C. M. Kelly, S. M. Crawford, C. A. Wheaton, O. L. Sydora, B. L. Small, M. Stradiotto, L. Turculet, *Organometallics* **2013**, *32*, 5581–5588; i) Q. Niu, H. Sun, X. Li, H. F. Klein, U. Florke, *Organometallics* **2013**, *32*, 5235–5238; j) V. K. Chidara, G. Du, *Organometallics* **2013**, *32*, 5034–5037; k) V. Cesar, L. C. Misal Castro, T. Dombay, J.-B. Sortais, C. Darcel, S. Labat, K. Miqueu, J. M. Sotiropoulos, R. Brousses, N. Lugan, G. Lavigne, *Organometallics* **2013**, *32*, 4643–4655; l) S. J. Kraft, R. H. Sanchez, A. S. Hock, *ACS Catal.* **2013**, *3*, 826–830; m) J. Zheng, S. Elangovan, D. A. Valyaev, R. Brousses, V. César, J.-B. Sortais, C. Darcel, N. Lugan, G. Lavigne, *Adv. Synth. Catal.* **2014**, *356*, 1093–1097; n) H. Zhao, H. Sun, X. Li, *Organometallics* **2014**, *33*, 3535–3539; o) Z. Zuo, H. Sun, L. Wang, X. Li, *Dalton Trans.* **2014**, *43*, 11716–11722; p) D. Kumar, A. P. Prakasham, L. P. Bheeter, J.-B. Sortais, M. Gangwar, T. Roisnel, A. C. Kalita, C. Darcel, P. Ghosh, *J. Organomet. Chem.* **2014**, *762*, 81–87; q) H. Zhou, H. Sun, S. Zhang, X. Li, *Organometallics* **2015**, *34*, 1479–1486; r) F. S. Wekesa, R. Arias-Ugarte, L. Kong, Z. Sumner, G. P. McGovern, M. Findlater, *Organometallics* **2015**, *34*, 5051–5056; s) M. A. Nesbit, D. L. M. Suess, J. C. Peters, *Organometallics* **2015**, *34*, 4741–4752; t) C. Ghosh, T. K. Mukhopadhyay, M. Flores, T. L. Groy, R. J. Trovitch, *Inorg. Chem.* **2015**, *54*, 10398–10406; u) B. Xue, H. Sun, X. Li, *RSC Adv.* **2015**, *5*, 52000–52006; v) S. Huang, H. Zhao, X. Li, L. Wang, H. Sun, *RSC Adv.* **2015**, *5*, 15660–15667; w) Y. Wei, S.-X. Liu, H. Mueller-Bunz, M. Albrecht, *ACS Catal.* **2016**, *6*, 8192–8200; x) T. C. Jung, G. Argouarch, P. van de Weghe, *Catal. Commun.* **2016**, *78*, 52–54; y) M. Rocquin, V. Ritleng, S. Barroso, A. M. Martins, M. J. Chetcuti, *J. Organomet. Chem.* **2016**, *808*, 57–62; z) X. Yu, F. Zhu, D. Bu, H. Lei, *RSC Adv.* **2017**, *7*, 15321–15329; aa) B. Xue, H. Sun, Q. Niu, X. Li, O. Fuhr, D. Fenske, *Catal. Commun.* **2017**, *94*, 23–28; ab) S. Ren, S. Xie, T. Zheng, Y. Wang, S. Xu, B. Xue, X. Li, H. Sun, O. Fuhr, D. Fenske, *Dalton Trans.* **2018**, *47*, 4352–4359; ac) Y. Li, J. A. Krause, H. Guan, *Organometallics* **2018**, *37*, 2147–2158; ad) X. Yang, C. Wang, *Chem. Asian J.* **2018**, *13*, 2307–2315; ae) X. Frogneux, F. Borondics, S. Lefrançois, F. D'Accrisio, C. Sanchez, S. Carencio, *Catal. Sci. Technol.* **2018**, *8*, 5073–5080; af) F. Ritter, D. Mukherjee, T. P. Spaniol, A. Hoffmann, J. Okuda, *Angew. Chem. Int. Ed.* **2019**, *58*, 1818–1822; ag) D. G. A. Verhoeven, J. Kwakemaak, M. A. C. van Wiggan, M. Lutz, M.-E. Moret, *Eur. J. Inorg. Chem.* **2019**, 660–667; ah) Á. Raya-Barón, P. Oña-Burgos, I. Fernández, *ACS Catal.* **2019**, *9*, 5400–5417; ai) O. Martínez-Ferraté, B. Chatterjee, C. Werlé, W. Leitner, *Catal. Sci. Technol.* **2019**, *9*, 6370–6378; aj) M. R. Elsby, R. T. Baker, *Chem. Commun.* **2019**, 55, 13574–13577; ak) K. Kobayashi, D. Taguchi, T. Moriuchi, H. Nakazawa, *ChemCatChem* **2020**, *12*, 736–739; al) C. K. Blasius, H. Wadepohl, L. H. Gade, *Eur. J. Inorg. Chem.* **2020**, 2335–2342; am) B. Royo, E. Peris, *Eur. J. Inorg. Chem.* **2012**, 1309–1318; b) L. Benítez Junquera, F. E. Fernández, M. C. Puerta, P. Valerga, *Eur. J. Inorg. Chem.* **2017**, 2547–2556.
- [5] a) M. Henrion, A. M. Oertel, V. Ritleng, M. J. Chetcuti, *Chem. Commun.* **2013**, *49*, 6424–6426; b) B. de P. Cardoso, J.-M. Bernard-Schaaf, S. Shahane, L. F. Veiros, M. J. Chetcuti, V. Ritleng, *Dalton Trans.* **2018**, *47*, 1535–1547.
- [6] F. Ulm, A. I. Poblador-Bahamonde, S. Choppin, S. Bellemin-Lapponnaz, M. J. Chetcuti, T. Achard, V. Ritleng, *Dalton Trans.* **2018**, *47*, 17134–17145.
- [7] a) A. A. D. Tulloch, A. A. Danopoulos, S. Winston, S. Kleinhenz, G. Eastham, *J. Chem. Soc., Dalton Trans.* **2000**, 4499–4506; b) S. Warsink, C. M. S. van Aubel, J. J. Weigand, S.-T. Liu, C. J. Elsevier, *Eur. J. Inorg. Chem.* **2010**, 5556–5562.
- [8] a) C. D. Abernethy, A. H. Cowley, R. A. Jones, *J. Organomet. Chem.* **2000**, *596*, 3–5; b) R. A. Kelly III, N. M. Scott, S. Díez-González, E. D. Stevens, S. P. Nolan, *Organometallics* **2005**, *24*, 3442–3447; c) V. Ritleng, C. Barth, E. Brenner, S. Milosevic, M. J. Chetcuti, *Organometallics* **2008**, *27*, 4223–4228; d) A. M. Oertel, J. Freudenreich, J. Gein, V. Ritleng, L. F. Veiros, M. J. Chetcuti, *Organometallics* **2011**, *30*, 3400–3411; e) Ł. Banach, P. A. Guńka, J. Zachara, W. Buchowicz, *Coord. Chem. Rev.* **2019**, *389*, 19–58.
- [9] CCDC 2081215 (**2a**) and CCDC 2081216 (**2b**) contain the supplementary crystallographic data which can be obtained free of charge via <https://www.ccdc.cam.ac.uk/structures/>.
- [10] H. S. Gutowsky, C. H. Holm, *J. Chem. Phys.* **1956**, *25*, 1228–1234.
- [11] V. Ritleng, A. M. Oertel, M. J. Chetcuti, *Dalton Trans.* **2010**, *39*, 8153–8160.
- [12] a) G. J. Martin, M. L. Martin, J. P. Gouesnard, *¹⁵N-NMR spectroscopy in NMR basic principles and progress*, Vol. 18 (Eds.: P. Diehl, E. Flick, R. Kosfeld), Springer-Verlag, Berlin, **1981**, pp. 75–186; b) S. Berger, S. Braun, H.-O. Kalinowski, *NMR spectroscopy of the non-metallic elements*, Wiley, Chichester, **1997**.
- [13] a) S. H. Strauss, *Chem. Rev.* **1993**, *93*, 927–942; b) S. P. Smidt, N. Zimmermann, M. Studer, A. Pfaltz, *Chem. Eur. J.* **2004**, *10*, 4685–4693; c) Y. Schramm, F. Barrios-Landeros, A. Pfaltz, *Chem. Sci.* **2013**, *4*, 2760–2766, and references therein.
- [14] a) J. H. Docherty, J. Peng, A. P. Dominey, S. P. Thomas, *Nat. Chem.* **2017**, *9*, 595–600; b) J. Peng, S. P. Thomas, *Synlett* **2020**, *31*, 1140–1146.
- [15] V. M. Chernyshev, O. V. Khazipov, M. A. Shevchenko, A. Y. Chernenko, A. V. Astakhov, D. B. Eremin, D. V. Pasyukov, A. S. Kashin, V. P. Ananikov, *Chem. Sci.* **2018**, *9*, 5564–5577.
- [16] For the hydrosilylation of sterically hindered ketones to alcohols, see: a) B. Tao, G. C. Fu, *Angew. Chem. Int. Ed.* **2002**, *41*, 3892–3894; *Angew. Chem.* **2002**, *114*, 4048–4050; b) D. A. Evans, F. E. Michael, J. S. Tedrow, K. R. Campos, *J. Am. Chem. Soc.* **2003**, *125*, 3534–3543; c) B. H. Lipshutz, C. C. Caires, P. Kuipers, W. Chrisman, *Org. Lett.* **2003**, *5*, 3085–3088; d) S. Díez-González, H. Kaur, F. K. Zinn, E. D. Stevens, S. P. Nolan, *J. Org. Chem.* **2005**, *70*, 4784–4796; e) S. Díez-González, N. M. Scott, S. P. Nolan, *Organometallics* **2006**, *25*, 2355–2358; f) G. Hamasaka, A. Ochida, K. Hara, M. Sawamura, *Angew. Chem. Int. Ed.* **2007**, *46*, 5381–5383; *Angew. Chem.* **2007**, *119*, 5477–5479; g) T.

- Fujihara, K. Semba, J. Terao, Y. Tsuji, *Angew. Chem. Int. Ed.* **2010**, *49*, 1472–1476; *Angew. Chem.* **2010**, *122*, 1514–1518.
- [18] F. Ulm, Y. Cornaton, J.-P. Djukic, M. J. Chetcuti, V. Ritleng, *Chem. Eur. J.* **2020**, *26*, 8916–8925.
- [19] L. P. Bheeter, M. Henrion, M. J. Chetcuti, C. Darcel, V. Ritleng, J.-B. Sortais, *Catal. Sci. Technol.* **2013**, *3*, 3111–3116.
- [20] S. Pelties, D. Herrmann, B. de Bruin, F. Hartl, R. Wolf, *Chem. Commun.* **2014**, *50*, 7014–7016.
- [21] R. H. Crabtree, *Chem. Rev.* **2012**, *112*, 1536–1554.
- [22] V. Papaefthimiou, D. K. Niakolas, F. Paloukis, T. Dintzer, S. Zafeiratos, *ChemPhysChem* **2017**, *18*, 164–170.
- [23] a) J.-F. Soule, H. Miyamura, S. Kobayashi, *J. Am. Chem. Soc.* **2013**, *135*, 10602–10605; b) M. Díaz de los Bernardos, S. Pérez-Rodríguez, A. Gual, C. Claver, C. Godard, *Chem. Commun.* **2017**, *53*, 7894–7897.
- [24] V. M. Chernyshev, E. A. Denisova, D. B. Eremin, V. P. Ananikov, *Chem. Sci.* **2020**, *11*, 6957–6977.

